Coupled quadratic boost converter for stand-alone PV applications

Suvamit Chakraborty, Amod C. Umarikar
Department of Electrical Engineering, Indian Institute of Technology Indore, Indore, India

Article Info	ABSTRACT
	This study focuses on a stand-alone photovoltaic (PV) system employing a high step-up quadratic boost converter and a battery management system. The quadratic boost converter, featuring a tapped inductor, facilitates voltage boosting by adjusting the duty ratio, ensuring low voltage stress on the active switch and enhancing overall efficiency. Coordination control techniques are proposed for smooth power transfer between the PV array, battery, and DC-link, accommodating variations in solar irradiation, ambient temperature, and loads. Design, modeling, and simulation are conducted using the PLEXSIM platform, and a real-time laboratory prototype validates system performance. This integrated approach establishes the feasibility and effectiveness of the proposed system, offering a robust framework for off-grid or rural electrification applications with its ability to operate at low voltage levels, efficient power transfer, and stable performance under uncertain conditions. *This is an open access article under the [CC BY-SA](#) license.*

Corresponding Author:

Suvamit Chakraborty
Department of Electrical Engineering, Indian Institute of Technology Indore
Indore, India
Email: phd1501202008@iiti.ac.in

1. INTRODUCTION

Non-conventional energy sources like photovoltaic (PV) and fuel cells have gained significant popularity in the power generation sector. However, these energy sources typically operate at low voltage levels, which necessitates voltage boosting for practical applications and compatibility with AC and DC loads. Stand-alone or off-grid systems are designed to cater to various applications such as solar lanterns, solar cells, street-lighting systems, solar water pumping, and stand-alone power plants in remote areas where grid electricity is not available [1], [2]. When it comes to stand-alone PV systems, different configurations have been proposed in the literature [3]-[6]. These configurations integrate PV panels, battery storage, and loads. However, many of these systems involve multiple conversion stages, resulting in a higher number of controlled switches. While some single-stage configurations have been reported in the literature, most of them do not include energy storage elements. The absence of an energy storage element in these configurations limits their ability to supply power to day-to-day household appliances. This is because achieving both maximum power point tracking (MPPT) operation and load voltage control becomes challenging without the presence of an energy storage element, such as a battery. Therefore, the inclusion of energy storage elements becomes essential in stand-alone PV systems to ensure optimal operation, efficient power utilization, and the ability to meet the demands of household appliances. By incorporating energy storage, it becomes feasible to achieve MPPT operation, regulate the load voltage, and provide a continuous power supply, even when the PV output fluctuates or is not available.

The bidirectional converter in the system serves an important role in facilitating bidirectional power flow between the PV source and the battery. Its ability to operate as both a buck and boost converter allows it to

adapt to the specific power flow requirements of the system at any given time. When the battery needs to be charged, the bidirectional converter operates as a boost converter, stepping up the voltage from the PV source to match the battery voltage and deliver power to the battery. This charging process enables energy storage for later use. Conversely, when the battery is discharging and supplying power to the load, the bidirectional converter operates as a buck converter. It steps down the battery voltage to match the load voltage and delivers power from the battery to the load. By dynamically switching between buck and boost modes, the bidirectional converter enables efficient bidirectional power flow, ensuring that the system can effectively utilize the energy from the PV source to charge the battery and deliver power to the load as needed. This flexibility and control over power flow direction are crucial for the proper functioning of a stand-alone PV system with battery storage.

In stand-alone PV systems, the solar energy generation sources typically have low output voltage levels. To interface these sources with the inverter and meet the voltage requirements of the system, high step-up DC-DC converters are necessary. Various high step-up converters have been developed for this purpose, incorporating switched capacitors or switched inductors to achieve high voltage conversion ratios. Some examples of high step-up DC-DC converters include:

- Hybrid boost converter [7]: This converter utilizes a combination of inductors and capacitors to achieve high voltage conversion. The voltage conversion ratio of the hybrid boost converter is $(1+D)/(1-D)$, where D represents the duty ratio.
- Switched-capacitor-based active network converter [8]: This converter employs switched capacitors to achieve high voltage conversion. The voltage conversion ratio of the switched-capacitor-based active network converter is $(3+D)/(1-D)$, where D is the duty ratio.
- Z-source and Quasi Z-source DC-DC converter [9]: These converters utilize impedance networks (Z-source or Quasi Z-source) to achieve high voltage conversion. The voltage conversion ratio of these converters is $(1-D)/(1-2D)$, where D represents the duty ratio.

However, the output voltages of these converters are floating, meaning they are not referenced to a fixed potential. In contrast, in a proposed solution presented in [10], the quadratic boost converter is introduced. This converter offers low buffer capacitor stress and achieves a voltage conversion ratio of $1/(1-D)2$, where D is the duty ratio. The quadratic boost converter provides a fixed output voltage with a reduced stress on the buffer capacitor.

These different converter topologies and configurations enable high voltage conversion in stand-alone PV systems, allowing efficient integration of the PV sources with the load and inverter systems. In the context of achieving high step-up voltage gain in stand-alone PV systems, different converter topologies have been proposed in the literature. One such approach is the coupled inductor-based converter, which offers high voltage gain. However, it is associated with challenges such as leakage energy, increased switching losses, and electromagnetic interference (EMI) issues. To mitigate these problems, an active clamp circuit can be employed. Another approach is the use of two cascade boost converters to achieve high voltage gain. However, this configuration introduces additional switches, leading to reduced efficiency.

On the other hand, the quadratic boost converter is a reliable option that offers a wide conversion range and requires only a single driver circuit [1]. Although structurally similar to cascaded boost converters, the quadratic boost converter provides improved performance. Tapped inductor-based boost converters have also been utilized for high-gain operation. While these converters can achieve high voltage gain, they often experience highly pulsating input current, especially when the turns ratio is high or the current is large. However, it has been observed that tapped-boost converters exhibit lower switch voltage stress compared to standard boost converters for the same output voltage. To address the power supply issue when PV power is unavailable, additional considerations need to be made. To effectively control the battery current in a quadratic-boost converter, which is crucial in a stand-alone system, a bidirectional DC-DC converter is integrated into the system. This converter enables efficient regulation of the battery charging and discharging processes. In summary, the proposed topologies in the references combine quadratic boost converters and tapped inductor boost converters to achieve high voltage gain in stand-alone PV systems. These configurations aim to overcome challenges related to voltage stress, switching losses, and input current pulsations. However, the references do not provide detailed analysis regarding power supply in the absence of PV power, and a bidirectional DC-DC converter is incorporated to control the battery current effectively.

Rural electrification through PV-based stand-alone systems is gaining popularity due to its ability to provide independent and reliable power generation. These systems are typically designed with low voltage levels for both the PV array and the battery, typically in the range of 24-36 V. Figure 1 shows a typical stand-alone PV system. However, to provide a suitable DC-link voltage for an inverter and enable a 230 V AC supply at the load terminal, a high voltage gain is required for the overall system. The design of the DC-DC converter plays a crucial role as it determines the efficiency, size, and weight of the converter. The low voltage provided by the PV array results in high currents in the primary part of the DC-DC converter. These high currents lead

to increased conduction and switching losses in the semiconductor devices, which can reduce the overall efficiency of the system.

Additionally, the requirement for a large voltage boost factor poses a significant challenge for the design of the DC-DC converter. To address these challenges, the use of a quadratic boost converter with a tapped inductor can be beneficial. The quadratic boost converter offers advantages such as higher voltage gain, improved efficiency, and reduced stress on the semiconductor devices. By incorporating a tapped inductor, the converter can achieve a higher voltage gain while mitigating the losses associated with high currents. This approach helps in optimizing the performance of the stand-alone PV system and overcoming the issues related to low voltage levels and high voltage boost requirements. Overall, the utilization of a quadratic boost converter with a tapped inductor presents a viable solution for rural electrification through stand-alone PV systems, offering improved efficiency, reduced losses, and effective power generation in areas with limited access to grid electricity.

The basic concept of the mentioned scheme incorporating a quadratic boost converter and its very preliminary study have been presented in the paper [1]. This work explores the use of a quadratic boost converter for a standalone PV system. Further, a control algorithm is developed for this topology which is simple and has an efficient control structure ensuring proper operating mode selection and smooth transition between different possible operating modes.

This paper is organized as follows. In section 2, the basic system overview and operation principle of the proposed quadratic boost converter are described. Section 3 describes the working principles and different modes of operation. In section 4, the basic control structure for the proposed quadratic boost standalone converter is presented, and some places simulations are given in the section. The hardware circuit is designed, and some experimental results are also presented for validation in this section. Finally, some concluding remarks and comments are given in section 5.
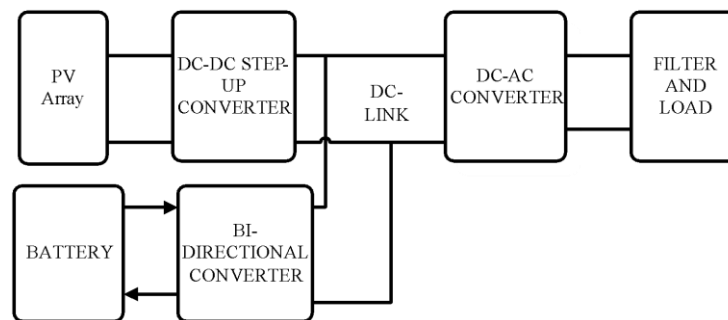

Figure 1. A typical standalone system

2.   QUADRATIC-BOOST CONVERTER WITH COUPLED INDUCTOR

In the field of PV-based standalone systems, two main converter structures have been widely explored: isolated converters and non-isolated converters. This paper specifically focuses on non-isolated PV DC stand-alone schemes, as there is room for improvement in this area. The boost converter is the most commonly used type of converter to achieve voltage gain in PV systems. However, researchers have made modifications to the boost converter design to achieve even higher voltage gains. One approach is the use of cascaded boost converters, where two boost converters are connected in series to provide a significant step-up voltage gain. However, this configuration requires the engagement of two switches, which can lead to reduced efficiency.

In contrast, the quadratic boost converter, despite its basic similarity to the cascaded boost converter, offers a more dependable solution with a single driver circuit [11]-[17]. The quadratic boost converter [1] utilizes a quadratic voltage conversion ratio, allowing for a wide conversion range. Researchers have further improved the voltage gain capability by developing tapped inductor-based quadratic boost converters as shown in Figure 2. These tapped inductor-based quadratic boost converters have been the focus of various studies and research efforts, aiming to enhance the voltage gain and overall performance of PV-based standalone systems [18]. By leveraging these advancements, the proposed system in this paper aims to address the limitations of existing non-isolated PV standalone systems and improve their efficiency and voltage conversion capabilities.

In Figure 3, a semi-tapped quadratic boost converter is depicted, which consists of an untapped inductor L1 and a tapped inductor CL. The primary purpose of this converter is to step up the typically low voltage generated by the PV system to a higher voltage level suitable for inverters or other DC applications. The quadratic boost converter, similar to the boost converter, utilizes a single active switch S1, and the converter's performance is evaluated based on the switch's condition. During the ON state of the switch, diode D2 becomes forward biased while diodes D1 and D3 become reverse biased. Inductor L1 and capacitor C1 are

charged by the supply voltage, while inductor CL is charged by capacitor C1. Conversely, during the OFF state of the switch, diode D2 becomes reverse biased, and diodes D1 and D3 become forward biased. Capacitors C1 and C2 are charged by the supply voltage and the inductors (L1 and CL), respectively. The operation conditions of the converter are illustrated in Figure 4, which provides a visual representation of the switch states and the charging/discharging of the various components (inductors and capacitors) during the ON and OFF states of the switch. Overall, the semi-tapped quadratic boost converter offers a means to step up the system's low voltage output, utilizing a quadratic boost technique and a single active switch for efficient voltage conversion.
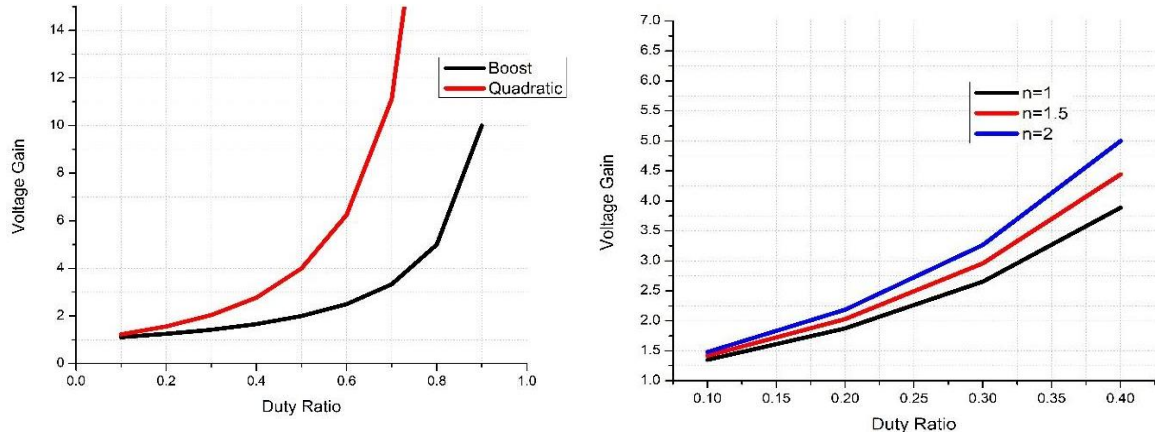
Figure 2. Duty ratio vs voltage gain graph of boost and quadratic boost converter and with different values of n
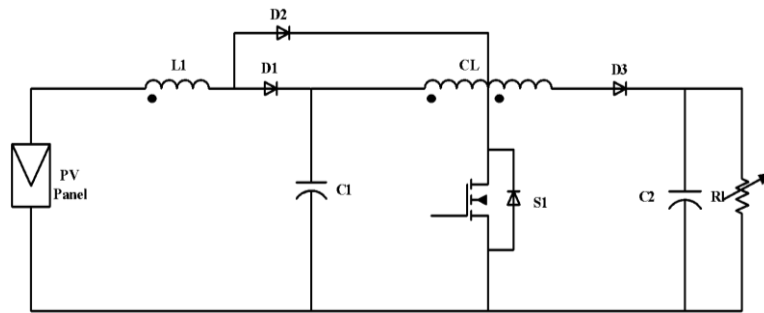
Figure 3. A typical PV-based quadratic boost converter with coupled inductor CL

The relationships of the capacitor voltages are given by (1) and (2).

$$V_c = \frac{V_{in}}{(1-2D)} \tag{1}$$

$$V_{c2} = \frac{V_{in}}{(1-D)^2} \tag{2}$$

Since the inductor L2 is tapped, then the output voltage becomes the function of the turn's ratio n of the tapped inductor, and it significantly boosts the voltage. The output voltage Vc2 and inductor current IL1 can be written as (3) and (4) respectively.

$$V_{c2} = \frac{V_{in}(1+nD)}{(1-D)^2} \tag{3}$$

$$I_{L1} = I_{in} = \frac{V_{in}(1+nD)^2}{R(1-D)^4} = \frac{V_o(1+nD)}{R(1-D)^2} \tag{4}$$

Where D is the shoot-through duty ratio. The current ripple ΔI_L1 of the inductor L1 can be written as (5).

$$\Delta I_{L1} = \frac{V_{in}DT_s}{L_1} \tag{5}$$

To obtain the ripple component for ΔI_L1, the inductance of L1 must satisfy the (6).

$$L_1 > \frac{V_{in}D}{\Delta I_L f_s} \tag{6}$$

Similarly, to obtain the ripple component for ΔI_CL, the inductance of CL must satisfy the (7).

$$L_{CL} > \frac{V_{in}D}{(1-D)\Delta I_{CL} f_s} \tag{7}$$

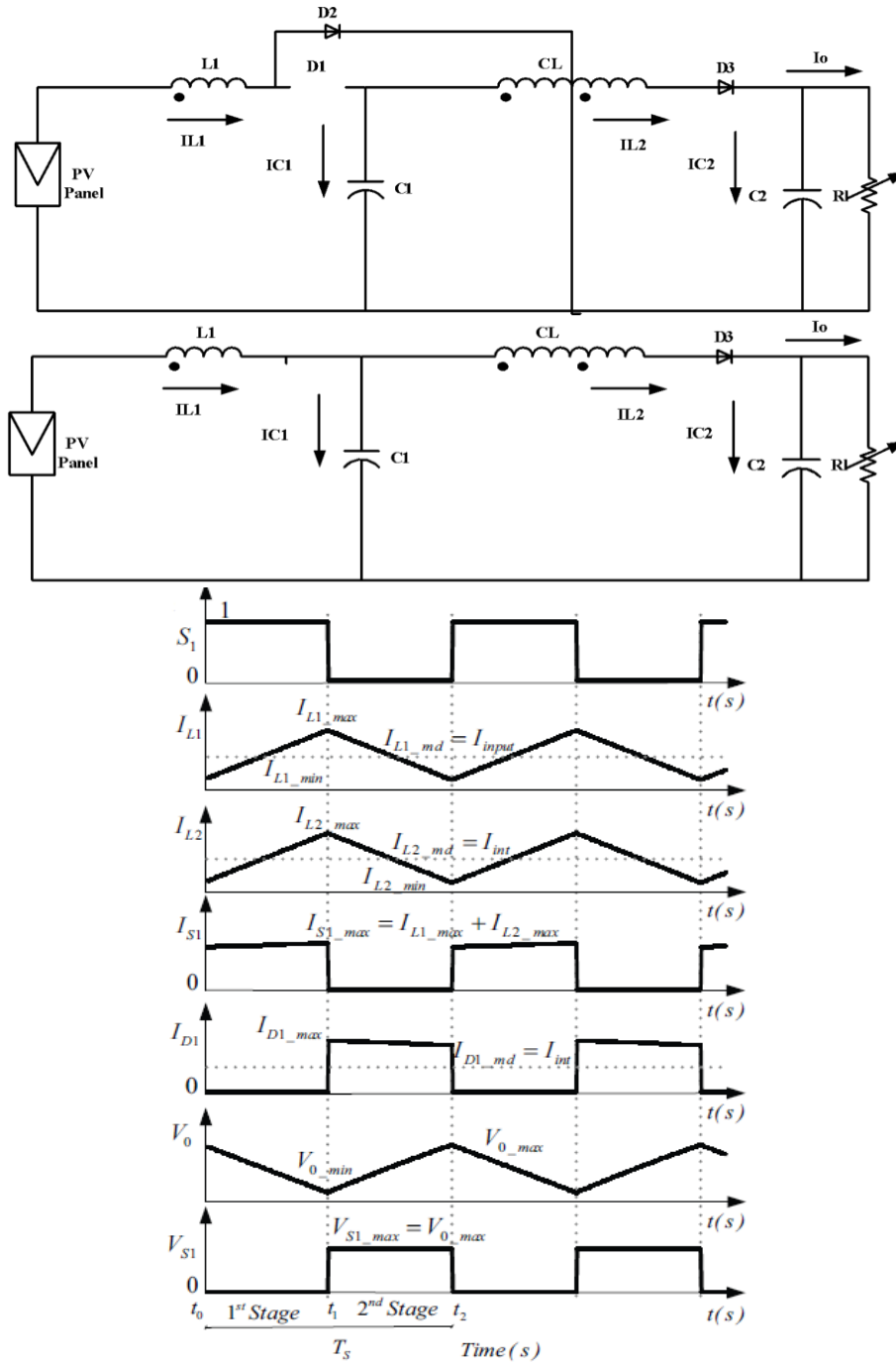The leakage inductance L_k is not considered as its value is negligible.

Figure 4. Quadratic boost converter when switch S1 is on and off and waveforms in CCM

3. PROPOSED SYSTEM

In the proposed standalone PV system shown in Figure 5, the quadratic boost converter plays a crucial role in boosting the output voltage. The converter operates similarly to the one described in reference [1], where it was observed that the output voltage is determined by the turns ratio (n) of the coupled inductor, allowing for significant voltage amplification. One major advantage of this converter is its ability to maintain continuous input current, as the input inductor is not tapped. This ensures smooth power transfer and efficient operation of the system. To interface the battery with the system, a bi-directional DC-DC converter is employed. This converter enables effective battery charging and discharging, providing control over the battery's energy flow. Careful control of battery charging and discharging is essential to preserve battery life and health, ensuring optimal performance and longevity. Overall, the proposed system integrates PV modules, a quadratic boost converter for voltage boosting, and a bi-directional DC-DC converter for battery interfacing. This design allows for efficient power management, effective battery control, and the provision of stable voltage levels required by the DC loads.
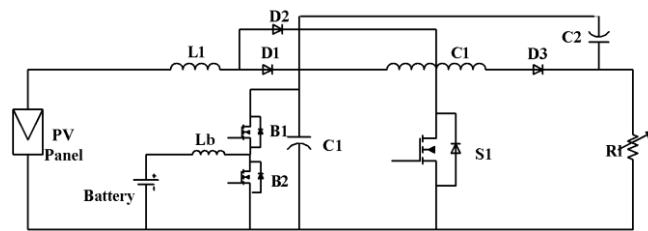

Figure 5. Proposed standalone PV system with battery

3.1. Principles of operation and modes analysis

The power flow of the system in a standalone PV system [18]-[20] can be categorized into the following scenarios:

- PV to load-battery fully charged: In this scenario, the PV array generates power and directly supplies it to the load without involving the battery. The battery is already fully charged and not actively involved in the power transfer.
- PV to battery-no load condition, battery charging: when there is no load or the load demand is low, the surplus power generated by the PV array is used to charge the battery. The PV power is directed towards the battery to replenish its energy storage.
- PV to both load and battery-surplus PV energy: when the PV array generates more power than what is required by the load, the excess power is used to simultaneously supply the load and charge the battery. This ensures efficient utilization of the surplus PV energy.
- PV and battery to load-deficit in PV energy: If the PV array alone cannot meet the power demand of the load, the battery is utilized to provide the remaining power required. The PV array supplies power to the load, and if necessary, the battery also contributes to meeting the load demand.
- Battery to load-insufficient PV power: In situations where the PV array is unable to generate sufficient power to meet the load demand, the battery takes over and supplies power to the load. The battery acts as an energy source to bridge the gap between the load demand and the available PV power.
- Worst case scenario - PV and DC bus to Battery: This mode is activated when the battery's state of charge (SoC) is low, and the PV source alone cannot provide the required charging current to the battery. In this case, the system shuts down as the PV power and the DC bus power are utilized to charge the battery and restore its energy level.

These power flow scenarios represent different operating conditions of the system based on the availability of PV power, load demand, and the state of the battery. The system intelligently manages the power flow to ensure efficient utilization of the PV energy and uninterrupted power supply to the load. This is shown in Figure 6.

3.2. Basic control structure and mode selection

- MPPT mode: In this mode, the system utilizes maximum power from the PV array. When the power generated by the PV source is greater than the load requirement, the excess power is used to simultaneously supply the load and charge the battery. The power balance equation in MPPT mode is given by $P\_pv + P\_bat = P\_load$, where P_pv represents the power generated by the PV source, P_bat represents the power

flowing into the battery, and P_load represents the power consumed by the load. The system remains in MPPT mode until the battery current (IB) is below a specified value determined by the State of Charge (SOC) of the battery. This ensures that the battery is not overcharged.

- Non-MPPT mode: When the load demand is lower than the generated power and the battery charging current exceeds its limit, the system switches to non-MPPT mode. In this mode, the power balance equation P_pv + P_bat = P_load still holds, but P_bat becomes negative, indicating that the battery discharges to meet the load demand. The battery charging current is maintained at a predetermined value to prevent overcharging. The operating point in non-MPPT mode is generally on the decreasing slope of the PV curve, indicating a reduction in PV power to match the load demand.

- Battery mode: In the absence of PV power, the standalone system operates in battery mode. The system supplies power to the load solely from the battery, ensuring that the battery is not over-discharged. This mode allows the system to meet the load demand when there is no PV power available, without risking excessive discharge of the battery.

- These three modes enable the system to optimize power extraction from the PV array, prevent overcharging or over-discharging of the battery, and ensure continuous power supply to the load under varying conditions.
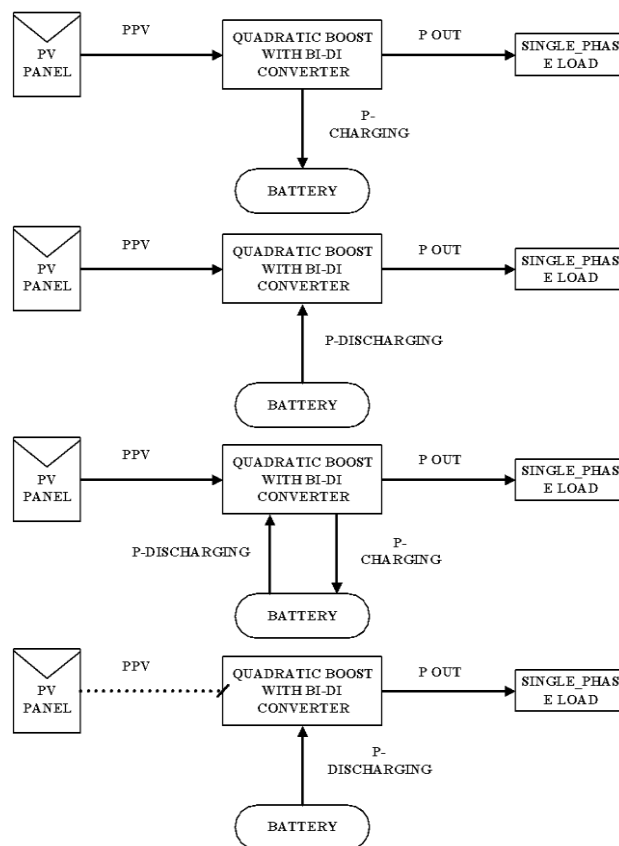

Figure 6. Different power flow operation of the proposed standalone PV system

3.3. Control of standalone modes

In the proposed standalone system, the control system is essential for determining the operating mode and managing power flow. The controller continuously monitors the system's current state and makes decisions based on power demand and the battery's specified state of charge (SOC). Figure 7 illustrates the MPPT algorithm used in this study, which is based on the perturb and observe method. In MPPT mode, as depicted in Figure 8, the controller adjusts the duty ratio to ensure maximum power extraction from the PV array.The MPPT block generates a reference current (Ipv-mpp) based on the desired operating point of the PV array. This reference current is compared with the actual PV current, and the error is passed through a PI controller. The output of the PI controller is the duty ratio (Dsh) for the switch of the quadratic boost converter, which regulates the PV current to track the maximum power point.

To control the DC-link voltage, the voltage across the capacitor C1 is measured and compared with the desired value. The error is then fed into a PI controller, which generates a current reference (Iref). This current reference is compared with the battery current (Ib), and the resulting error is used to generate the duty ratio (Db) for the bidirectional converter. The bidirectional converter allows power flow between the PV array and the battery, controlling the battery charging or discharging process.

When there is no PV energy available, the controller shifts the system to battery only mode to supply power to the load solely from the battery. The controller must continuously monitor the current state of the system, evaluating parameters that indicate power excess or deficit. Based on these parameters, the controller determines the appropriate mode of operation for the system. Overall, the control system in the proposed standalone system ensures efficient power management, optimal MPPT operation, battery charging/discharging control, and seamless power supply to the load under varying conditions.
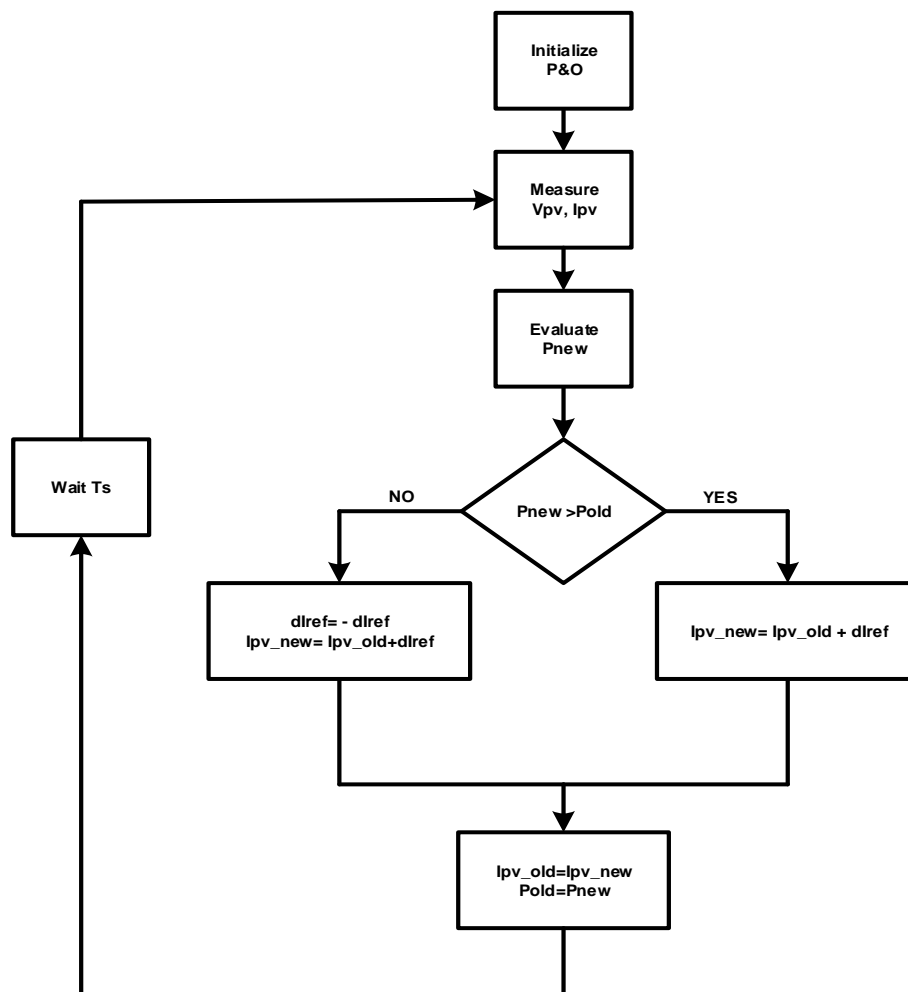

Figure 7. Flowchart of the P&O MPPT algorithm

The control strategy for the proposed standalone system involves monitoring and controlling the system in three different modes: MPPT mode, non-MPPT mode, and battery only (BO) mode. The system is designed to shift between these modes based on the operating conditions. In the non-MPPT mode shown in Figure 9, the reference current Iref is subtracted from the maximum battery current Ibmax to generate the reference PV current Ipvref. This reference current is used to regulate the voltage across the capacitor VC1, ensuring its maintenance within a certain voltage range. If there is a sudden change in the load, causing VC1 to fall below a specified voltage, the controller automatically shifts from the non-MPPT mode to the MPPT mode to optimize power extraction from the PV array. This transition allows the system to adapt to varying load conditions and improve overall performance.
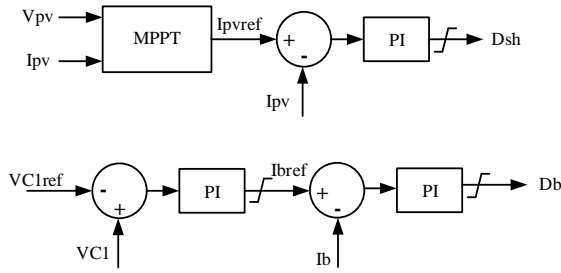
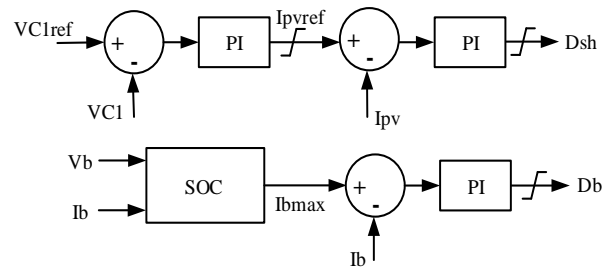Figure 8. Proposed operation mode in
the MPPT mode

Figure 9. Proposed operation mode in
the non-MPPT mode

When there is no PV energy available, the system enters the battery-only (BO) mode as shown in Figure 10. In this mode, the battery becomes the sole power source and is responsible for supplying the entire load. The operation in MPPT mode and BO mode is similar, with the exception that the MPPT controller remains idle in BO mode. The system maintains stable operation in the BO mode to ensure an uninterrupted power supply in the absence of PV energy.

To facilitate the control of different modes, four control signals, M, NM, BO, and Non-BO, are generated. When M=1 and NM=0, the controller operates the PV in MPPT mode, with the battery maintaining the DC-link voltage. If the load reduces or solar radiation increases, causing the battery current IB to reach Ibmax as specified by the state of charge (SOC), NM is set to 1 and M is set to 0. The controller then operates the battery in a constant current mode, maintaining the battery charging current at Ibmax, while the PV array takes responsibility for maintaining the DC-link voltage.

For BO=0 and non-BO=1, the controller operates the PV array in either MPPT mode or non-MPPT mode, depending on the status of M and NM. When BO=1 and non-BO=0, indicating the absence of PV energy, the controller shifts to the battery-only mode, where the battery maintains the DC-link voltage and supplies power to the load. This control strategy shown in Figure 11 allows the system to adapt to changing operating conditions and ensures efficient operation in all three modes, namely MPPT mode, non-MPPT mode, and BO mode. The control signals M, NM, BO, and non-BO enable the system to switch between these modes and disable the modes that are not required based on the prevailing conditions. Figure 12 shows the algorithm to identify and switch between different modes.
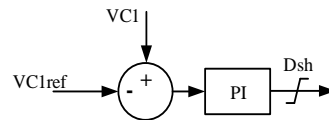

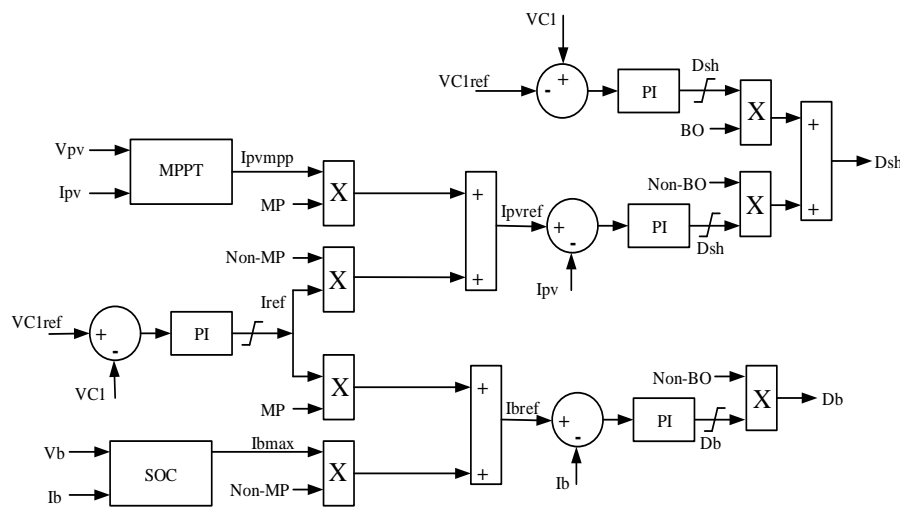Figure 10. Proposed operation mode in the battery-only mode

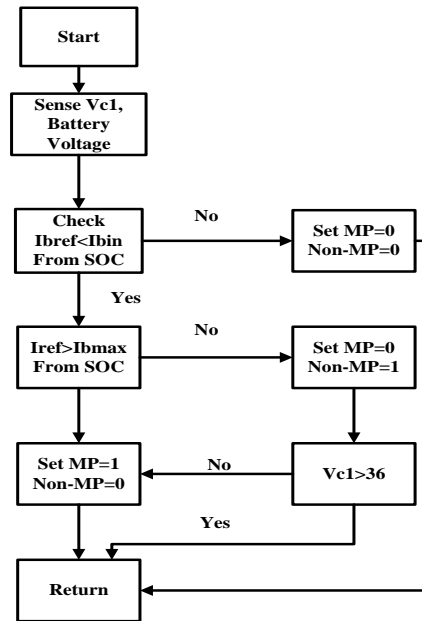Figure 11. Overall control strategy

Figure 12. Proposed operation mode identification strategy

4. SIMULATION AND EXPERIMENTAL RESULTS

4.1. Simulation result of proposed converter

The theoretical assumptions were validated through both simulation and experimental setups of the quadratic boost converter with a tapped inductor. Testing was conducted for both MPPT and non-MPPT modes under rated load and variable load conditions to ensure the performance of the system in different operating scenarios. The designed system was implemented using the simulation software PLECS, with a chosen switching frequency of 20 kHz. The PV operating range was set between 17 to 22 volts, with an open circuit voltage of 22 V and an MPP voltage of the selected PV panel at 17.6 V. The battery's nominal voltage was taken as 24 V. For MPPT operation, the perturb & observe (P&O) method was employed to extract the maximum power from the solar panel. This algorithm periodically perturbs the PV current with a small incremental step and compares the resulting power with the previously delivered power, allowing the system to track the maximum power point. Figure 13 shows the MPPT tracking by the quadratic boost converter through the Aplab solar emulator. To regulate the battery current, a conventional proportional-integral (PI) controller was used in the battery controller. This PI controller ensures that the battery charging and discharging currents are controlled within the specified limits, thereby protecting the battery and maintaining its state of charge (SOC). The tapped inductor used in the system has a turns ratio of 1.5, which contributes to achieving the desired high voltage gain. By conducting simulations and experimental tests, the performance and functionality of the proposed system were evaluated and validated. These results demonstrate the effectiveness of the quadratic boost converter with a tapped inductor topology in achieving the desired power conversion and control objectives.

4.2. Experimental result of proposed converter

To experimentally validate the proposed system, a laboratory prototype was developed shown in Figure 14. The switching frequency of the converter was chosen as 20 kHz, considering the trade-off between power density and efficiency. The battery bank was constructed by connecting two 12 V, 26 Ah batteries in series. This configuration provided the necessary voltage and capacity for the system's energy storage. To emulate the solar array, an AplabSAS120/10 ODIV solar array simulator was utilized. This simulator generates the P-V (power-voltage) and I-V (current-voltage) characteristics of the PV array based on four input parameters: Vmpp (maximum power point voltage), Voc (open-circuit voltage), Impp (maximum power point current), and Isc (short-circuit current) of the PV module. These parameters allow the simulator to mimic the behavior of a real solar array. The loads connected to the converter output were rheostats, which can be adjusted to vary the load conditions and evaluate the system's performance under different scenarios. The semiconductor devices employed in the laboratory prototype include: i) Quadratic and bi-directional switches: IRFP4668PbF (MOSFET); ii) Diode for PV panel, Dpv: MBR1535CT; and iii) Quadratic-diode, D: RHRG30120

These semiconductor devices were selected based on their specifications and suitability for the proposed system. The other relevant parameters and elements used in constructing the prototype were consistent with those employed in the simulation study. The details of these parameters can be found in Table 1 of the research documentation. By implementing the laboratory prototype and utilizing the specified components, the experimental validation of the proposed system was conducted, allowing for a practical assessment of its performance and functionality.

Table 1. Simulation and experimental parameters

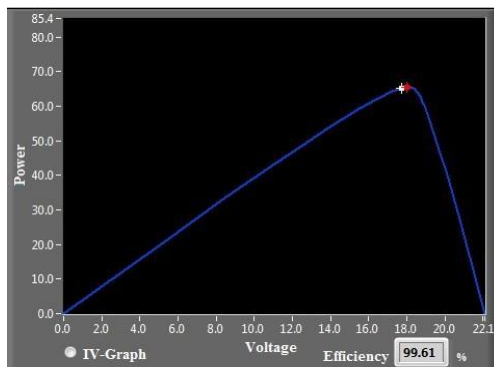| Parameters	Value	Parameters	Value
PV Input Voltage; Vdc(V)	17.5	Tapped turn Ratio	1.5
Switching Frequency fs (kHz)	20	Output Filter Capacitor Cf(µF)	10
Capacitors C1=C2(µF)	2200	Output Filter Inductor Lf (mH)	0.15
Inductor L1(mH)	1	Load Resistance R(ohm)	204
Inductor L2(mH)	1.5	Total power of the System(W)	65

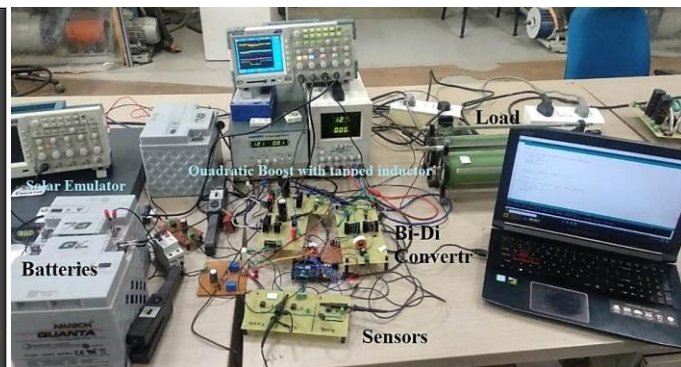Figure 13. MPPT tracking in AplabSAS120/10 ODIV solar emulator

Figure 14. Experimental setup of the proposed standalone system

The observation of spikes in switch voltages and inductor currents in the steady-state response of the system as shown in Figure 15 can indeed be attributed to the presence of leakage inductance. Leakage inductance refers to the imperfect coupling between the primary and secondary windings of a transformer or inductor. In an idealized analysis or simulation, the effects of leakage inductance are often neglected for simplicity. However, in practical implementations, the leakage inductance can introduce voltage spikes and current transients due to the energy stored in the leakage magnetic field. These spikes occur during switching transitions of the converter.

From Figure 16, it can be observed that the system is operating in the maximum power point (MPP) mode while negotiating a 65 W load. The MPP values for the PV array are set at Vmpp = 17.6 V and Impp = 3.69 A. It is evident from the graph that the PV voltage (Vpv) and current (Ipv) attain values equal to the set MPP values. This indicates that the system is successfully tracking and operating at the maximum power point of the PV array. Furthermore, the voltage at capacitor C1 (Vc1) is maintained around 48V, demonstrating the effectiveness of the system's voltage regulation. Similarly, the voltage at capacitor C2 (Vc2) is maintained at 95V, indicating stable voltage regulation at the output. Overall, the steady-state response of the system in MPP mode confirms that the PV voltage and current are maintained at their desired MPP values, while the voltages at capacitors C1 and C2 are regulated within the specified ranges.

In the second case, the PV array initially operates at the maximum power point (MPP) as determined by the MPPT algorithm. At t=2 sec, there is a step change in solar radiation from 1000 W/m2 to 800 W/m2, as shown in Figure 17. Despite this step change in solar radiation, it can be observed that the PV array continues to operate at its MPP. This is achieved through the control of the battery current, which adjusts to maintain the system in the MPP mode. By adjusting the battery current, the system ensures that the PV array operates at its maximum power point, maximizing the power extraction from the available solar energy. This control mechanism allows the system to adapt to changes in solar radiation and maintain optimal operation. Additionally, the voltage across capacitor C2 (Vc2) is maintained at a constant level of 95V, indicating the stability of the system's voltage regulation. Overall, the system demonstrates its ability to maintain the PV array at its MPP, even in the presence of step changes in solar radiation, while ensuring stable voltage regulation at Vc2.

In Figure 18, the performance of the system during the mode transition between maximum power point mpp (MPP) and non-MPP modes is illustrated. The system behavior is observed while the load demand

changes and affects the charging of the battery. Initially, the system is operating in the MPP mode with a load demand of 65 W, and the PV array is providing power to both the load and the battery charging. The MPP values for the PV array are Vmpp = 17.6 V and Impp = 3.69 A. During this period, the battery is being discharged. At a specific instant "t," the load demand is reduced to 30 W. As a result, the surplus power generated by the PV array starts charging the battery. The charging current of the battery gradually increases until it reaches the maximum allowable charging current set at 2 A. Once the battery charging current reaches the 2 A limit, the system transitions from the MPP mode to the non-MPP mode. This transition is observed in Figure 18, where it can be seen that when the battery charging current is restricted to 2 A, the PV array operates at a point other than its MPP. Consequently, the PV output power yield is reduced compared to its maximum potential. The PV power is obtained from the PV simulator display, which provides the P-V (power-voltage) and I-V (current-voltage) characteristics of the PV array. The battery voltage is measured using a multimeter to monitor its state during the mode transition. Figure 18 demonstrates the system's response to the change in load demand and the subsequent transition between MPP and non-MPP modes. This control mechanism ensures that the battery charging current does not exceed the specified limit while effectively utilizing the surplus power from the PV array for charging.
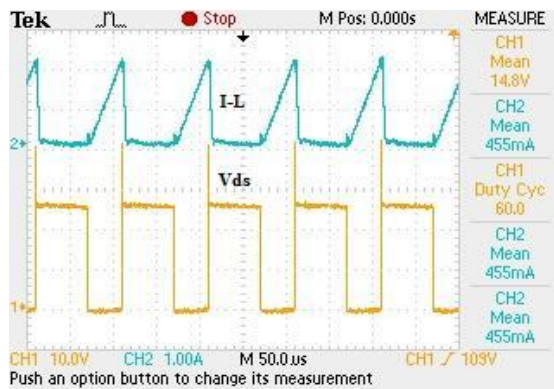

Figure 15. Experimental results voltage across switch and current through the tapped inductor
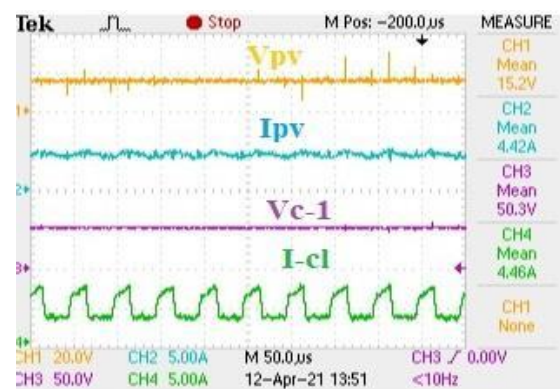

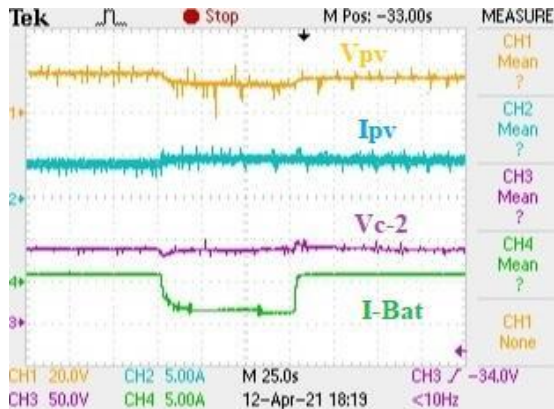Figure 16. Experimental results while operating in MPPT mode (steady state)

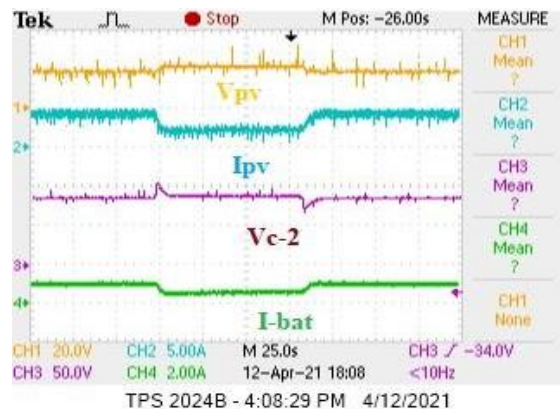Figure 17. MPPT mode during irradiation change from 1000 to 800W/m^2

Figure 18. Experimental results while transition from MPPT mode to non-MPPT mode

Figure 19 depicts the response of the system during the transition between the BO and maximum power point tracking (MPPT) modes. The behavior of the system is observed when the PV array is connected and disconnected from the system. Initially, the system is operating in the BO mode with Vmpp (PV voltage at MPP) and Impp (PV current at MPP) both set to 0. At the first instant, denoted as "t," the PV array is connected to the system. As a result, the PV voltage quickly reaches its maximum power point (MPP) value of 17.6 V, and the PV current reaches its corresponding MPP value of 3.69 A. The system transitions from the BO mode to the MPPT mode. During the MPPT mode, the PV voltage is tightly controlled at its MPP value of

17.6 V, as indicated in Figure 15. This control ensures that the maximum power is extracted from the PV array. Additionally, the voltage across the capacitor C2 (Vc2) is maintained at a constant value of 95V in both the MPPT and BO modes. At the second instant, also denoted as "t," the PV array is disconnected from the system. Consequently, the system transitions from the MPPT mode back to the BO mode. The PV voltage drops to 0 V, and the PV current decreases accordingly. Figure 19 demonstrates that the system successfully maintains the PV voltage at its MPP value during the MPPT mode, while also ensuring the stability of Vc2 throughout both the MPPT and BO modes. This smooth transition between modes allows for efficient utilization of the available solar energy and reliable power supply to the loads.

The efficiency of the quadratic boost converter, as measured from the laboratory prototype, is presented in Figure 20. The efficiency is calculated by dividing the load power by the sum of the PV power and battery power. The measurements are conducted using a power analyzer, PM100 for load power, PV simulator display for PV power, and a multimeter and ammeter for battery power.
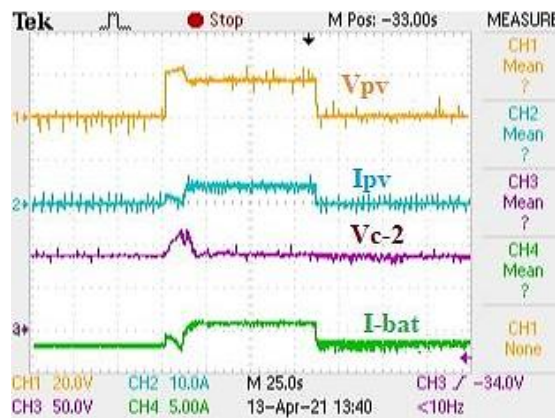

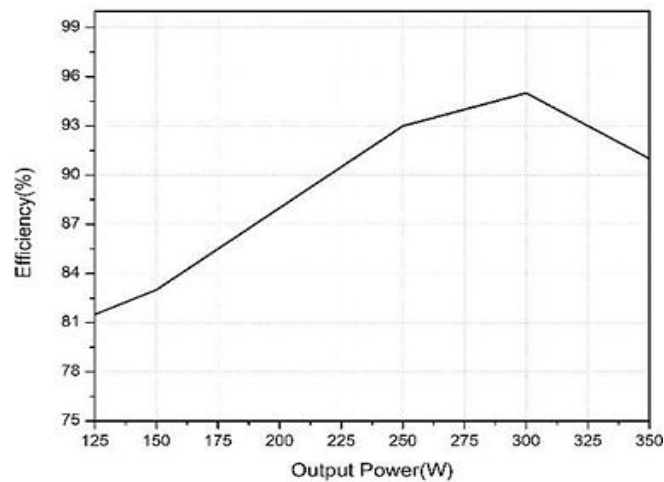Figure 19. Mode transition between battery-only mode to MPPT to battery-only

Figure 20. Efficiency plot of the proposed converter

Comparative experiments were also performed using a simple boost converter, which showed that the quadratic boost converter achieves a higher voltage gain of approximately 30% compared to the boost converter. Although a better comparison could be made with a cascaded boost converter, the quadratic boost converter still offers a higher output voltage at the same duty ratio.

The efficiency of the quadratic boost converter is reported to be higher than that of the boost converter, using the same devices. Additionally, the quadratic boost converter exhibits improved output ripple characteristics, which can even be canceled at certain duty ratio values. The quadratic boost converter is also said to have lower EMI due to power phase shifting. However, it is noted that controlling the quadratic boost converter is slightly more complicated than the boost converter.

Furthermore, the use of a quadratic boost converter allows for the utilization of smaller energy storage devices. The proposed system is compared with other standalone schemes mentioned in the literature, and Table 2 provides a comparison of various aspects and traits of these schemes. Based on these findings, it can be inferred that the proposed system utilizing the quadratic boost converter offers several benefits, including higher efficiency, improved output ripple, and reduced EMI compared to other schemes.

Table 2. Comparison of the proposed scheme with typical stand-alone systems

Scheme	No of stages	N_s	N_d	N_t	N_l	N_C	Dedicated converter for MPPT	No of converter in battery charging path
Chen et al. [21]	3	9	0	1	5	6	yes	2
Wang and Zhang [22]	4	7	5	0	4	4	yes	1
Chen et al. [23]	3	12	12	1	3	2	yes	2
Mutoh and Inoue [24]	4	#	#	1	#	#	yes	2
Debnath and Chatterjee [25]	2	6	2	1	3	6	no	1
Proposed	2	6	1	1	3	3	no	1

5. CONCLUSION

The paper introduces a solar PV-based stand-alone system that incorporates a non-isolated semi-tapped quadratic boost converter. This converter design offers improved voltage gain at lower duty ratios compared to other converter topologies such as quadratic-boost and boost converters. The analysis of steady-state conditions reveals that the semi-tapped quadratic boost converter achieves higher voltage gain for the same duty ratio. The voltage gain and voltage stress on the switch of the semi-tapped converter depends on the duty ratio and the turn ratio of the tapped inductor. The primary objective of the proposed system is to ensure smooth power transfer between the PV panel, batteries, and loads while maintaining stable voltages for DC electrical loads. The inclusion of a bi-directional DC-DC converter facilitates efficient battery charging and discharging. This approach allows for the utilization of low voltage levels for both the PV array and the battery, making it suitable for rural areas where low-voltage systems are prevalent.

The control structure of the overall stand-alone system is presented, showcasing the strategies for regulating power flow and maintaining stable voltages. Simulation studies are conducted to validate the effectiveness of the proposed control structure in achieving the desired performance. To further verify the system's performance, experimental tests are carried out using a laboratory prototype. These tests aim to validate the feasibility and practicality of the proposed system in real-world scenarios. The experimental results provide evidence of the system's capability to deliver the expected performance and validate the effectiveness of the control structure. In summary, the paper proposes a solar PV-based stand-alone system that employs a non-isolated semi-tapped quadratic boost converter. The system offers advantages such as higher voltage gain, adjustable battery charging and discharging, and operation at low voltage levels. The control structure is validated through simulations and experimental tests, demonstrating the system's feasibility and potential for practical applications.

REFERENCES

[1] K. Patidar and A. C. Umarikar, "High step-up converters based on quadratic boost converter for micro-inverter," *Electric Power Systems Research*, vol. 119, pp. 168–177, 2015, doi: 10.1016/j.epsr.2014.09.018.

[2] S. Chakraborty and A. Umarikar, "Standalone PV system based on Isolated Quasi Z-Source Converter," in *Proceedings of 2018 IEEE International Conference on Power Electronics, Drives and Energy Systems, PEDES 2018*, 2018. doi: 10.1109/PEDES.2018.8707527.

[3] N. Surulivel, D. Debnath, and C. Chakraborty, "A Novel Single Coupled-Inductor Boost TPC With Two Inductively Interfaced Ports Suitable for Renewable Energy Integration," *IEEE Transactions on Industrial Electronics*, vol. 70, no. 5, pp. 4705–4715, 2023, doi: 10.1109/TIE.2022.3187576.

[4] R. Chattopadhyay and K. Chatterjee, "PV based stand alone single phase power generating unit," in *IECON 2012 - 38th Annual Conference on IEEE Industrial Electronics Society*, IEEE, Oct. 2012, pp. 1138–1144. doi: 10.1109/IECON.2012.6388612.

[5] D. Vinnikov and I. Roasto, "Quasi-Z-Source-based isolated DC/DC converters for distributed power generation," *IEEE Transactions on Industrial Electronics*, vol. 58, no. 1, pp. 192–201, 2011, doi: 10.1109/TIE.2009.2039460.

[6] D. Debnath and K. Chatterjee, "Solar photovoltaic-based stand-alone scheme incorporating a new boost inverter," *IET Power Electronics*, vol. 9, no. 4, pp. 621–630, 2016, doi: 10.1049/iet-pel.2015.0112.

[7] B. Axelrod, Y. Berkovich, and A. Ioinovici, "Switched-capacitor/switched-inductor structures for getting transformerless hybrid DC-DC PWM converters," *IEEE Transactions on Circuits and Systems I: Regular Papers*, vol. 55, no. 2, pp. 687–696, 2008, doi: 10.1109/TCSI.2008.916403.

[8]   A. A. Fardoun and E. H. Ismail, "Ultra step-up DC-DC converter with reduced switch stress," *IEEE Transactions on Industry Applications*, vol. 46, no. 5, pp. 2025–2034, 2010, doi: 10.1109/TIA.2010.2058833.

[9]   V. P. Galigekere and M. K. Kazimierczuk, "Analysis of PWM Z-source DC-DC converter in CCM for steady state," *IEEE Transactions on Circuits and Systems I: Regular Papers*, vol. 59, no. 4, pp. 854–863, 2012, doi: 10.1109/TCSI.2011.2169742.

[10]   Y. M. Ye and K. W. E. Cheng, "Quadratic boost converter with low buffer capacitor stress," *IET Power Electronics*, vol. 7, no. 5, pp. 1162–1170, 2014, doi: 10.1049/iet-pel.2013.0205.

[11]   S. Peddapati and S. Naresh, "Quadratic Boost Converter for Green Energy Applications," in *DC—DC Converters for Future Renewable Energy Systems. Energy Systems in Electrical Engineering*, A. Priyadarshi, N., Bhoi, A.K., Bansal, R.C., Kalam, Ed., Springer, 2022, pp. 173–202. doi: 10.1007/978-981-16-4388-0_9.

[12]   Y. R. De Novaes, A. Rufer, and I. Barbi, "A new quadratic, three-level, DC/DC converter suitable for fuel cell applications," *Fourth Power Conversion Conference-NAGOYA, PCC-NAGOYA 2007 - Conference Proceedings*, pp. 601–607, 2007, doi: 10.1109/PCCON.2007.373028.

[13]   Y. Wang, Y. Qiu, Q. Bian, Y. Guan, and D. Xu, "A Single Switch Quadratic Boost High Step Up DC–DC Converter," *IEEE Transactions on Industrial Electronics*, vol. 66, no. 6, pp. 4387–4397, Jun. 2019, doi: 10.1109/TIE.2018.2860550.

[14]   P. Saadat and K. Abbaszadeh, "A Single-Switch High Step-Up DC-DC Converter Based on Quadratic Boost," *IEEE Transactions on Industrial Electronics*, vol. 63, no. 12, pp. 7733–7742, 2016, doi: 10.1109/TIE.2016.2590991.

[15]   D. Amudhavalli, N. K. Mohanty, and A. K. Sahoo, "Interleaved quadratic boost converter integrated with dickson voltage multiplier with energy storage for high power photo voltaic applications," *International Journal of Power Electronics and Drive Systems*, vol. 12, no. 2, pp. 957–967, 2021, doi: 10.11591/ijpeds.v12.i2.pp957-967.

[16]   R.-J. Wai and R.-Y. Duan, "High Step-Up Converter With Coupled-Inductor," *IEEE Transactions on Power Electronics*, vol. 20, no. 5, pp. 1025–1035, Sep. 2005, doi: 10.1109/TPEL.2005.854023.

[17]   Y. Li, S. Sathiakumar, and J. L. Soon, "Improved quadratic boost converter using switching coupled-inductor and voltage-doubler," *Australian Journal of Electrical and Electronics Engineering*, vol. 16, no. 1, pp. 33–45, 2019, doi: 10.1080/1448837X.2019.1589951.

[18]   T. F. Wu, Y. S. Lai, J. C. Hung, and Y. M. Chen, "Boost converter with coupled inductors and buck-boost type of active clamp," *IEEE Transactions on Industrial Electronics*, vol. 55, no. 1, pp. 154–162, 2008, doi: 10.1109/TIE.2007.903925.

[19]   M. Z. Zulkifli, M. Azri, A. Alias, N. Talib, and J. M. Lazi, "Simple control scheme buck-boost DC-DC converter for stand alone pv application system," *International Journal of Power Electronics and Drive Systems*, vol. 10, no. 2, pp. 1090–1101, 2019, doi: 10.11591/ijpeds.v10.i2.pp1090-1101.

[20]   M. Asim, A. Sarwar, M. Shahabuddin, and M. S. Manzar, "Development of solar photovoltaic model for wide range of operating conditions," *International Journal of Power Electronics and Drive Systems*, vol. 12, no. 4, pp. 2483–2491, 2021, doi: 10.11591/ijpeds.v12.i4.pp2483-2491.

[21]   Y. M. Chen, A. Q. Huang, and X. Yu, "A high step-up three-port DC-DC converter for stand-alone PV/battery power systems," *IEEE Transactions on Power Electronics*, vol. 28, no. 11, pp. 5049–5062, 2013, doi: 10.1109/TPEL.2013.2242491.

[22]   H. Wang and D. Zhang, "The stand-alone PV generation system with parallel battery charger," *Proceedings - International Conference on Electrical and Control Engineering, ICECE 2010*, pp. 4450–4453, 2010, doi: 10.1109/iCECE.2010.1083.

[23]   Y. M. Chen, Y. C. Liu, and F. Y. Wu, "Multi-input dc/dc converter based on the multiwinding transformer for renewable energy applications," *IEEE Transactions on Industry Applications*, vol. 38, no. 4, pp. 1096–1104, 2002, doi: 10.1109/TIA.2002.800776.

[24]   N. Mutoh and T. Inoue, "A control method to charge series-connected ultraelectric double-layer capacitors suitable for photovoltaic generation systems combining MPPT control method," *IEEE Transactions on Industrial Electronics*, vol. 54, no. 1, pp. 374–383, 2007, doi: 10.1109/TIE.2006.885149.

[25]   D. Debnath and K. Chatterjee, "Two-Stage Solar Photovoltaic-Based Stand-Alone Scheme Having Battery as Energy Storage Element for Rural Deployment," *IEEE Transactions on Industrial Electronics*, vol. 62, no. 7, pp. 4148–4157, 2015, doi: 10.1109/TIE.2014.2379584.

BIOGRAPHIES OF AUTHORS

Suvamit Chakraborty ⓘ 🖾 SC ◉ is a doctoral student in the Electrical Engineering Department at the Indian Institute of Technology, Indore. He is currently engaged in researchon various power topologies to be integrated in photovoltaic systems. He can be contacted at email: phd1501202008@iiti.ac.in.

Amod C. Umarikar ⓘ 🖾 SC ◉ is a professor in the Electrical Engineering Department at Indian Institute of Technology, Indore. His main research interests include applications of power electronics in renewable energy systems, power quality and smart grid. He can be contacted at email: umarikar@iiti.ac.in.